Organic & Biomolecular Chemistry

Cite this: *Org. Biomol. Chem.*, 2011, **9**, 5523

www.rsc.org/obc

PAPER

A naphthalene-based Al^{3+} selective fluorescent sensor for living cell imaging†

Animesh Sahana,[a] Arnab Banerjee,[a] Sudipta Das,[a] Sisir Lohar,[a] Debasis Karak,[a] Bidisha Sarkar,[b] Subhra Kanti Mukhopadhyay,[b] Asok K. Mukherjee*[a] and Debasis Das*[a]

Received 26th March 2011, Accepted 10th May 2011
DOI: 10.1039/c1ob05479a

An efficient fluorescent Al^{3+} receptor, *N*-(2-hydroxy-1-naphthalene)-*N*′-(2-(2-hydroxy-1-naphthalene)-amino-ethyl)-ethane-1,2-diamine (**L**) has been synthesized by the condensation reaction between 2-hydroxy naphthaldehyde and diethylenetriamine. High selectivity and affinity of **L** towards Al^{3+} in ethanol (EtOH) as well as in HEPES buffer at pH 7.4, makes it suitable to detect intracellular Al^{3+} with fluorescence microscopy. Metal ions, *viz.* Li^+, Na^+, K^+, Mg^{2+}, Ca^{2+}, Mn^{2+}, Co^{2+}, Ni^{2+}, Cu^{2+}, Zn^{2+}, Ag^+, Cd^{2+}, Hg^{2+} and Pb^{2+} do not interfere. The lowest detection limit for Al^{3+} is 3.0×10^{-7} M and 1.0×10^{-7} M in EtOH and HEPES buffer respectively.

Introduction

The toxicity of aluminum towards a variety of living beings including humans is well discussed in the literature.[1] For example, Al^{3+} toxicity causes bone and joint diseases, neuronal disorder leading to dementia, myopathy and Alzheimer's disease.[2] Aluminum is the third most abundant metal in the earth's crust, accounting for approximately 8% of its mass. Acid rain increases free Al^{3+} in surface water by leaching from soil. This is deadly to growing plants.[3] Although Al^{3+} is widely used in our daily life, it is a non-essential element for living systems. Its atomic size (0.051 nm) and electric charge (Al^{3+}) makes it a competitive inhibitor of several essential elements of similar characteristics such as Mg^{2+} (0.066 nm), Ca^{2+} (0.099 nm) and Fe^{3+} (0.064 nm). Aluminum is found in its ionic form in most animal and plant tissues as well as in natural waters. Main sources of Al^{3+} to accumulate on human beings are food additives, aluminum-based pharmaceuticals, occupational dusts, aluminum containers and cooking utensils. According to a WHO report the average daily human intake of aluminum is around 3–10 mg. Tolerable weekly aluminum dietary intake in the human body is estimated to be 7 mg kg^{-1} body weight.[4] Detection and estimation of Al^{3+} levels in the biosphere have a direct impact on human health. Development of fluorescent chemosensors has currently attracted significant interest because of their potential application in medicinal and environmental research. Amongst several methods for the detection of Al^{3+} in the literature,[5] spectrofluorimetry[6] is widely used for its high sensitivity, selectivity, rapidity and easy operational procedure. The poor coordination ability of Al^{3+} compared to the transition metal ions[7] makes the development of an Al^{3+} fluorosensor difficult. Several fluorescent probes such as hydrazones,[8] Schiff bases,[9] coumarin,[6] pyrollidine,[6] calixarene,[10] dipyrromethene,[6] hydroxyflavone,[11] 8-hydroxyquinoline,[12] oxazoline and imidazoline[13] derivatives have been synthesized and used for this purpose. Most of the reported Al^{3+} sensors suffer from interference caused by Fe^{3+} and Cu^{2+},[14] poor water solubility and tedious synthetic methods of preparation.[15] Metal complexes of Schiff bases[16] have been widely studied due to their anti-tumor properties,[17] antioxidant activities,[18] attractive electronic and photophysical properties.[19] Naphthalene has been chosen as an ideal component of a fluorescent chemosensor due to its short fluorescence lifetime,[20] low fluorescence quantum yield[21] and ability to act as a donor as well as an acceptor.[22] Hydrophilic functionalities should be incorporated along with the naphthalene moiety to design a water-soluble Al^{3+} selective fluorescent sensor. The present study is aimed to serve these purposes to develop an efficient water-soluble Al^{3+} sensor for imaging living cells at physiological pH.

Herein, we report the synthesis and characterization of a Schiff base ligand (**L**) obtained by condensing 2-hydroxy naphthaldehyde with diethylenetriamine. It is used as an efficient fluorescent probe for the determination of Al^{3+} in EtOH as well as in HEPES buffer (0.1 M) solution (pH 7.4). Trace level detection of Al^{3+} in living cells was performed.

Results and discussion

Scheme 1 shows the facile one step synthesis of the ligand **L**. Its molecular structure and purity was established from different spectroscopic studies like ^{1}H NMR, MS and FTIR (Fig. S1, Fig. S2 and Fig. S4 respectively, ESI†). It is well known that performance of a fluorescence sensor based on an electron donor/acceptor mechanism is highly dependent on the concentration of protons in the medium as they compete with the metal ion of interest to bind with the ligand. Thus optimization of the pH to increase the efficiency of the sensor is essential. Fluorescence pH titrations

[a]*Department of Chemistry, The University of Burdwan, Burdwan, -713104, West Bengal, India. E-mail: ddas100in@yahoo.com; Fax: +91-342-2530452; Tel: +91-342-2533913*
[b]*Department of Microbiology, The University of Burdwan, Burdwan, -713104, West Bengal, India*

† Electronic supplementary information (ESI) available. See DOI: 10.1039/c1ob05479a

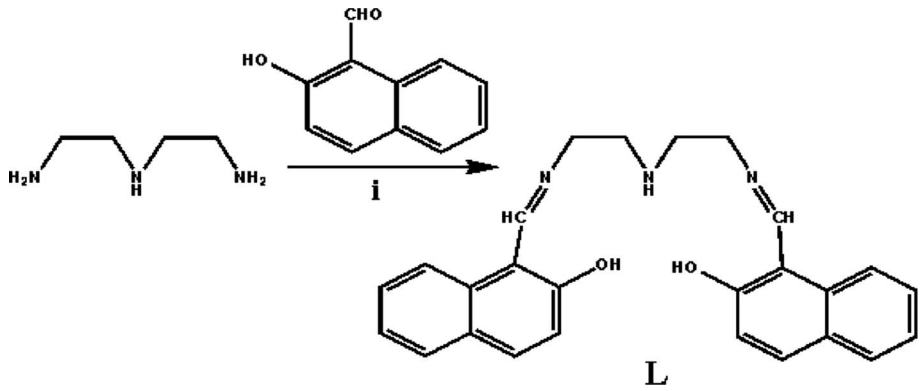

Scheme 1 Synthesis of the ligand, **L**. Conditions: (i) reflux for 8 h in ethanol.

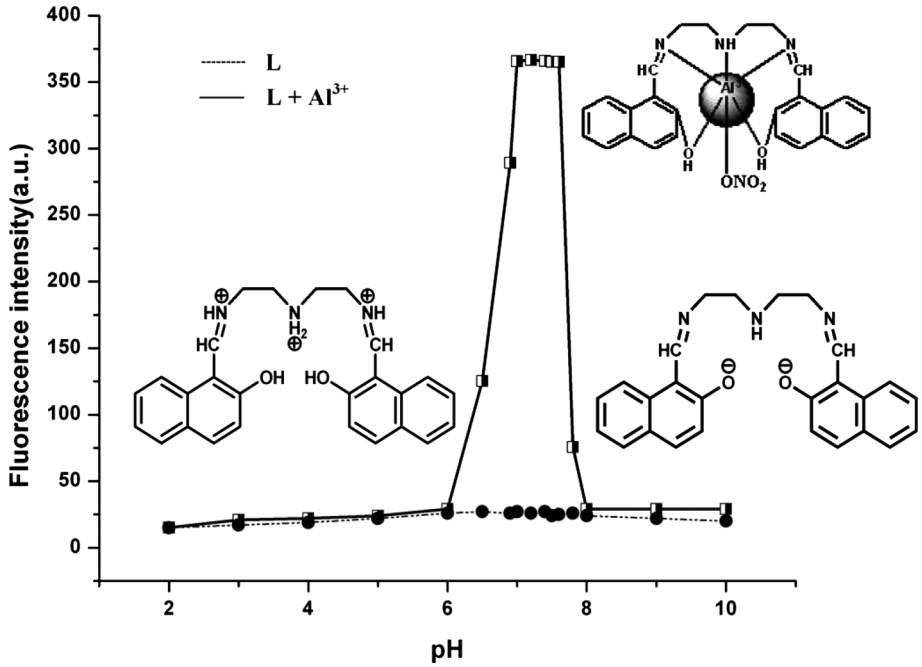

Fig. 1 Effect of pH on the binding efficiency of **L** (10 μM) towards Al^{3+} (1.0 equivalent) in HEPES buffer (0.1 M), (ethanol/water = 3/7, v/v) (λ_{em}: 445 nm, λ_{ex}: 355 nm).

were carried out for this purpose. Equimolar amounts of **L** and Al^{3+} were mixed in different sets of pH (pH 2.0–10.0). Fig. 1 clearly demonstrates that at the pH range from 7.0 to 7.4, the **L**–Al^{3+} system showed maximum emission intensity. Fluorescence emission intensities of **L** remain unchanged on addition of Al^{3+} at a pH below 6.5 and above 7.4. Most plausibly, protonation of **L** at a pH below 6.5, prevented coordination of Al^{3+}. On the other hand, at a pH above 7.4, OH^- may succeed against **L** in binding to Al^{3+}.

The fluorescence spectral properties of **L** (10 μM) were investigated both in EtOH (Fig. 2) and in 0.1 M HEPES buffer at pH 7.4 (ethanol/water = 3/7, v/v, Fig. 3) as a function of added [Al^{3+}]. The fluorescence emission band of **L** at 445 nm is very weak at room temperature with a quantum yield 14.2×10^{-3}. Addition of Al^{3+} (10 μM) to **L** (10 μM) in HEPES buffer solution at pH 7.4 afforded a 13.5 fold enhancement in fluorescence intensity with a 4.14 times increase in fluorescence quantum yield (58.8×10^{-3}) (ESI†). In the absence of Al^{3+} ions, the extent of intramolecular charge transfer (ICT) in **L** was sufficient enough to quench its fluorescence. The chelation of **L** with Al^{3+} not only reduced the ICT effect[6] in **L** but also increased the rigidity of the molecular assembly by restricting the free rotations of the azomethine carbon with respect to the naphthalene ring resulting in a significant enhancement of the fluorescence intensity which is known as chelation-enhanced fluorescence (CHEF).[6] Metal ions (20 equivalent) such as Li^+, Na^+, Mg^{2+}, K^+, Ca^{2+}, Mn^{2+}, Co^{2+}, Ni^{2+}, Fe^{3+}, Cu^{2+}, Zn^{2+}, Ag^+, Cd^{2+}, Hg^{2+} and Pb^{2+} failed to behave like Al^{3+} with the ligand **L** (Fig. 4). From Fig. 5, we observed that there was no interference for detection of Al^{3+} in the presence of Li^+, Na^+, K^+, Mg^{2+}, Ca^{2+}, Mn^{2+}, Co^{2+}, Ni^{2+}, Cu^{2+}, Zn^{2+}, Ag^+, Cd^{2+}, Hg^{2+} and Pb^{2+}. In the case of Fe^{3+}, quenching of the fluorescence signal was observed. In the presence of a mixture containing various cations *viz.*, Zn^{2+}, Mn^{2+}, Co^{2+}, Ni^{2+}, Cd^{2+}, Hg^{2+}, Pb^{2+}, designated as **Mix** in Fig. 5, together with Al^{3+}, an almost similar fluorescence enhancement was observed that was previously shown by the Al^{3+} ion itself. This unique selectivity of **L** towards Al^{3+} could be interpreted in

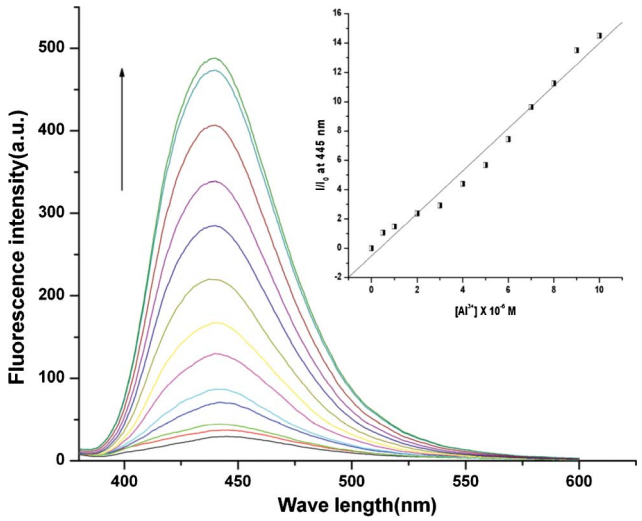

Fig. 2 Fluorescence spectra of the ligand (**L**) (10 μM) as a function of externally added [Al^{3+}]. From bottom to top: [Al^{3+}] = 0, 0.5, 1, 2, 3, 4, 5, 6, 7, 8, 9, 10,12,14,15,18 μM. Inset: Plot of the fluorescence intensity of **L** (10 μM) as a function of externally added [Al^{3+}] up to 10 μM. [solvent = ethanol, λ_{em}: 445 nm, λ_{ex}: 355 nm].

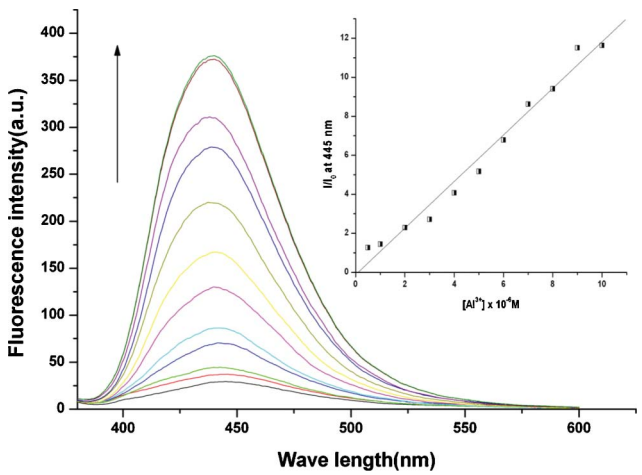

Fig. 3 Fluorescence spectra of the ligand (**L**) (10 μM) as a function of externally added [Al^{3+}]. From bottom to top: [Al^{3+}] = 0, 0.5, 1, 2, 3, 4, 5, 6, 7, 8, 9, 10 μM in HEPES buffer (0.1 M), (medium: ethanol/water = 3/7, v/v, pH 7.4). Inset: Plot of fluorescence intensity of **L** (10 μM) as a function of externally added [Al^{3+}]. λ_{em}: 445 nm, λ_{ex}: 355 nm.

terms of the smaller ionic radii (0.5 Å) and higher charge density ($r = 4.81$) of the Al^{3+} ion. The smaller radii of the Al^{3+} ion permits a suitable coordination geometry of the chelating receptor **L** and the larger charge density allows a strong coordination ability between **L** and Al^{3+}.

The plot of fluorescence intensities *vs.* externally added [Al^{3+}] (inset Fig. 2 and Fig. 3) revealed that above 10 μM of Al^{3+}, there was no further change in the emission intensity of the system. Using the calibration graph (inset of Fig. 2 and 3), it was possible to determine [Al^{3+}] in ethanol or HEPES buffer solution up to 10 μM. In both ethanol and HEPES buffered ethanol–water media the calibration curve is linear with a correlation coefficient, R^2 = 0.99. The detection limit was determined from the fluorescence titration data based on a reported and broadly used method.[6,23]

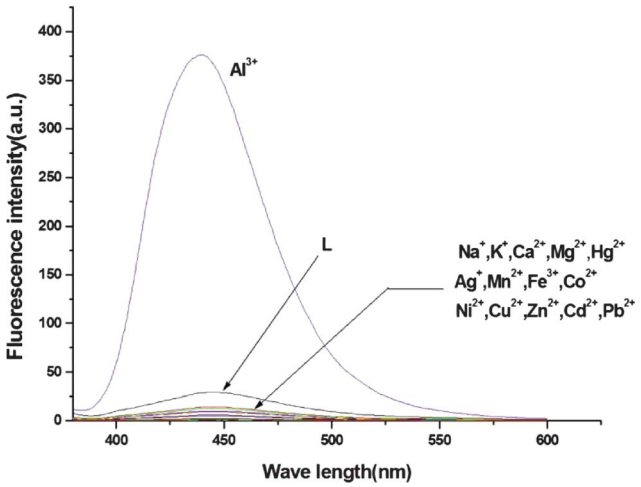

Fig. 4 Fluorescence spectra of **L** (10 μM), **L** + Al^{3+} (10 μM) and **L**(10 μM) + M (200 μM), where M = Na^+, K^+, Ca^{2+}, Mg^{2+}, Ag^+, Mn^{2+}, Hg^{2+}, Fe^{3+}, Co^{2+}, Ni^{2+}, Cu^{2+}, Zn^{2+}, Cd^{2+} and Pb^{2+} (λ_{em}: 445 nm, λ_{ex}: 355 nm, HEPES buffer).

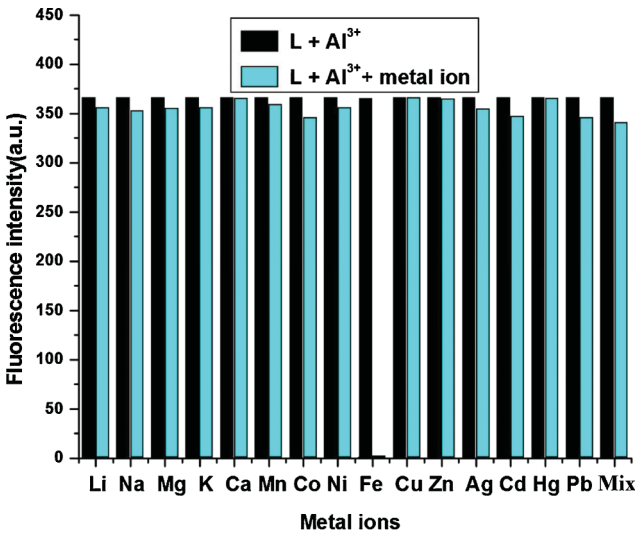

Fig. 5 Interference from other metal cations in a binary mixture: **L** (10 μM) + Al^{3+} (10 μM) + M^{n+} (200 μM), where M^{n+} = Li^+, Na^+, K^+, Mg^{2+}, Ca^{2+}, Mn^{2+}, Co^{2+}, Ni^{2+}, Fe^{3+} Cu^{2+}, Zn^{2+}, Ag^+, Cd^{2+}, Hg^{2+} and Pb^{2+}. **Mix** = (Zn^{2+}, Mn^{2+}, Co^{2+}, Ni^{2+}, Cd^{2+}, Hg^{2+}, Pb^{2+}) were present together with **L** and Al^{3+} (λ_{em}: 445 nm, λ_{ex}: 355 nm, HEPES buffer).

According to the result of the titration experiment, the fluorescent intensity data at 445 nm were normalized between the minimum intensity (0.0 equivalent free Al^{3+}) and the maximum intensity and are displayed in Fig. 2 and Fig. 3. A linear regression curve was then fitted to these normalized fluorescent intensity data, and the point at which this line crossed the ordinate axis was considered as the detection limit. We could detect [Al^{3+}] as low as 3.0×10^{-7} M (Fig. S5, ESI†) and 1.0×10^{-7} M (Fig. S6, ESI†) in ethanol and 0.1 M HEPES buffer solution respectively (**L** = 10 μM) which are much below the acceptable limit of [Al^{3+}] (0.05 mg L^{-1} or 1.85 μM) in drinking water. Thus the present method could be applied to determine trace level [Al^{3+}] in drinking water.

Changes in the fluorescence intensity of **L** upon binding with Al^{3+} were monitored in various other solvents like methanol, acetone, *N*,*N*-dimethylformamide (DMF), dimethyl

sulfoxide (DMSO), acetone, acetonitrile, toluene, chloroform and dichloromethane. From Fig. 6, it was evident that except methanol and ethanol, no other solvent was promising.

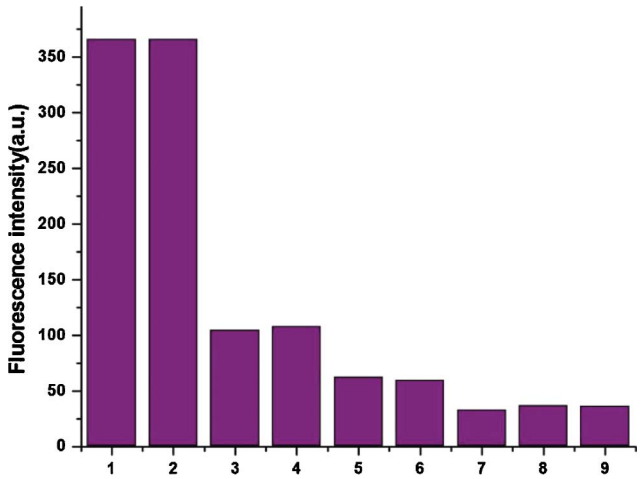

Fig. 6 Fluorescence intensities of **L** + Al^{3+} (10 μM/10 μM) in different solvents. 1: methanol/water (3/7) (v/v); 2: ethanol/water(3/7) (v/v); 3: DMF, 4: DMSO, 5: acetonitrile; 6: chloroform; 7: acetone; 8: dichloromethane; 9: toluene.

Fig. 7 illustrates the change in the UV-Vis spectra of **L** (10 μM) in 0.1 M HEPES buffer (ethanol/water = 3/7, v/v, pH 7.4) on addition of Al^{3+}. The absorption spectrum of **L** showed one intense absorption band at 232 nm, which was attributed to the C═N bond. The absorbance of this band increased upon addition of Al^{3+} indicating coordination of azomethine N to Al^{3+}. Moreover the appearance of two new peaks at 205 nm and 317 nm indicated the formation of the **L**–Al^{3+} complex. The intensity of the absorption band of **L** at 245 nm and 278 nm increased on complex formation. Fig. 7 also shows that there is a gradual decrease in intensity of absorption in the range 375–450 nm. In fact the free ligand is yellow coloured, giving an absorption band between 375–450 nm. When an equivalent quantity of Al^{3+} is added, this band decreases in intensity (Fig. S13, ESI†). However,

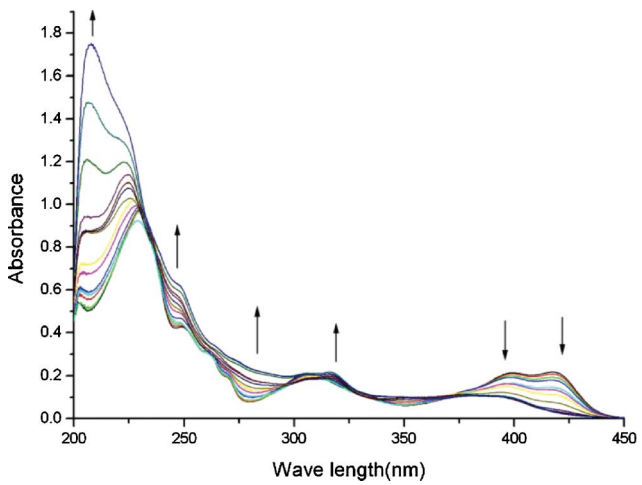

Fig. 7 Changes in the absorption spectra of **L** (10 μM) upon addition of 0.5, 1, 1.5, 2, 2.5, 3, 3.5, 4, 5, 6, 7, 8, 9,10 μM of Al^{3+} in HEPES buffer (0.1 M, ethanol/water = 3/7, v/v, pH 7.4).

deprotonation on complexation does not occur, as is evident from NMR, mass spectrum and variation of fluorescence intensity with pH. The probable reason is that before complexation, the oxygen lone pairs of electrons take part in long π-conjugation, but after complexation they are bound to Al^{3+}, thereby intercepting the conjugation.

Changes in the intensities of the absorption peaks of **L** (10 μM) on addition of 1 and 10 equivalent of Al^{3+} are shown in Fig. S14, ESI†.

A Job plot indicated a 1 : 1 stoichiometry of the complex formed between **L** and Al^{3+} (Fig. S7, ESI†), which was corroborated by the mass spectra of Al^{3+}–**L** complex. Using Li's equations, the binding constant of **L** with Al^{3+} in HEPES buffer (Fig.S8, ESI†) was determined.[6] The binding constant value of 2.12×10^5 M^{-1} ($R^2 = 0.987$) indicated a significant strong binding between **L** and Al^{3+}. The response parameter α, which was defined as the ratio of the free ligand concentration to the initial concentration of the ligand, was plotted as a function of the added Al^{3+} concentration (Fig. 8). This plot could also be used as the calibration curve for determination of unknown Al^{3+}. So **L** could be used in chelation therapy as a remedy from Al^{3+} toxicity.

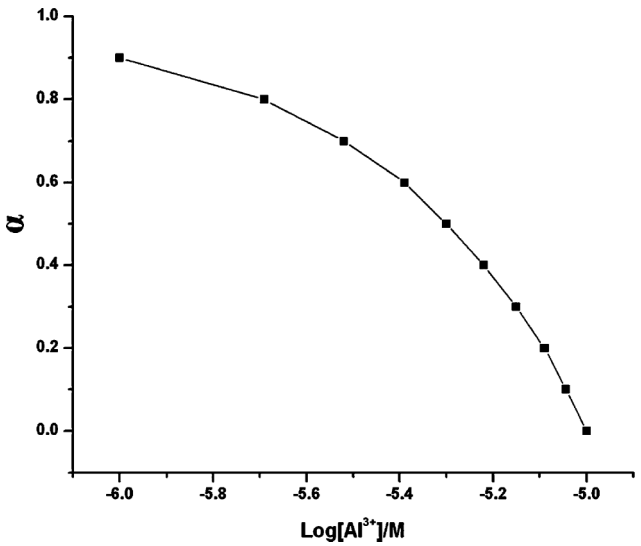

Fig. 8 Response parameter (α) as a function of the log[Al^{3+}]. $\alpha = [\mathbf{L}]_{t=t}/[\mathbf{L}]_{t=0}$ in HEPES buffer (0.1 M), (ethanol/water = 3/7, v/v).

From the ESI†, mass (Fig. S3, ESI†), FTIR (Fig. S9, ESI†) and ^{1}H NMR spectra (Fig. S10, ESI†) of the **L**–Al^{3+} complex, we proposed the composition of the final product, **L**–Al^{3+} complex as shown in Fig. 9. Literature reported on the coordination number of Al^{3+} in most Al complexes[24] helped us to conclude the present Al^{3+}–**L** complex. A Job plot (Fig. S7, ESI†) (Al^{3+} : **L** = 1 : 1) corroborated our conclusion. The peaks at $m/z = 523.19$ (calculated, 523.15) and $m/z = 434.21$ (calculated, 434.18) corresponded to Al**L**(NO_3) (Fig. S3, ESI†) and **L** (Fig. S2, ESI†), respectively.

In order to strengthen our conclusion based on the findings through UV-Vis and fluorescence spectroscopy, we performed ^{1}H NMR titrations by the concomitant addition of Al^{3+} (as its nitrate salt) to the DMSO-d_6 solution of **L**. Significant spectral changes were observed in the ^{1}H NMR spectra of **L** upon the addition of Al^{3+} as shown in Fig. 10. Results are presented in Table S1 (ESI†). Relative to the free **L**, all the protons of the **L**–Al^{3+} complex

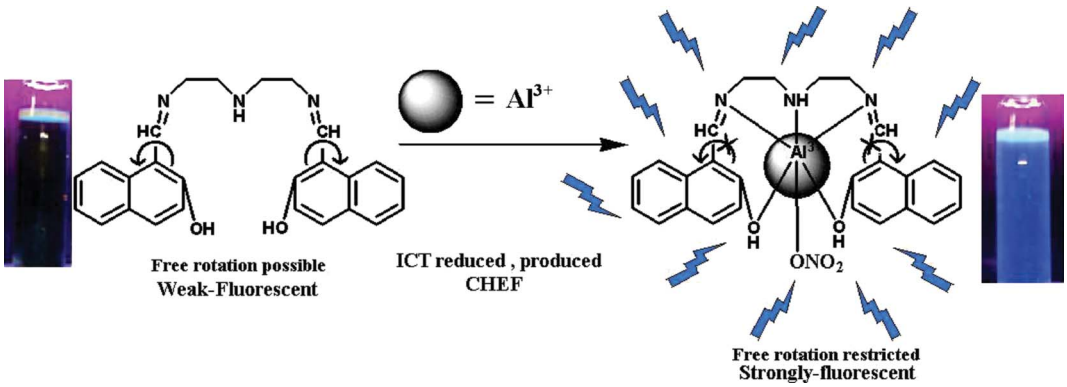

Fig. 9 Proposed mechanism (CHEF) for the fluorescent sensing of **L** to Al^{3+}.

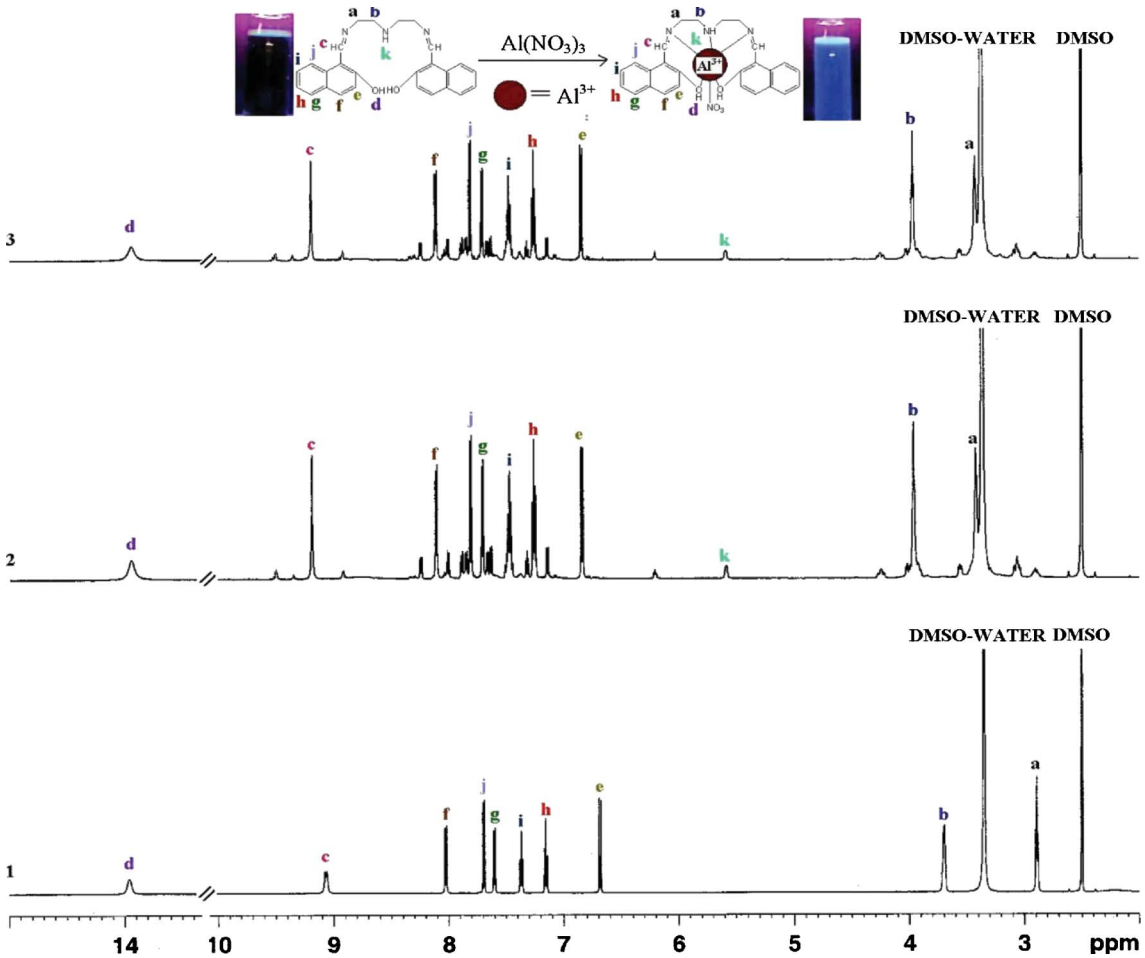

Fig. 10 Binding mode of **L**–Al^{3+} and ^{1}H NMR spectra of **L** with $Al(NO_3)_3{\cdot}9H_2O$ in DMSO-d_6: (1) **L**; (2) **L** with 1 equiv. of Al^{3+} (3) **L** with 1.5 equiv. of Al^{3+}.

resonate slightly in the downfield region. Azomethine protons in the free **L** corresponded to a doublet signal but changed to a singlet after the addition of Al^{3+}. This might be attributed to the fact that the flexibility (the free rotation of the azomethine carbon with respect to naphthalene ring) which was present in **L** brought two H atoms (labeled as c and j) close enough for coupling but in the **L**–Al^{3+} complex the free rotation was restricted, keeping these two H atoms far apart (Fig. 10). The N–H signal which was absent in free **L** appeared at δ 5.6 after the addition of Al^{3+}. This fact suggested the involvement of the nitrogen lone pair to bind Al^{3+} which rendered N–H non-exchangeable (also evidenced from the broadness of the δ 5.6 signal). The same type of broadening of the O–H signal (δ 13.9) in the Al^{3+} complex was also observed.

Finally, thermogravimetric studies of the free **L** (Fig. S11, ESI†) and **L**–Al^{3+}complex (Fig. S12, ESI†) provided further support in favor of efficient binding of the **L** with Al^{3+}. While **L** was found to be stable up to 200 °C, the thermal stability of the **L**–Al^{3+} complex was much less (135 °C only).

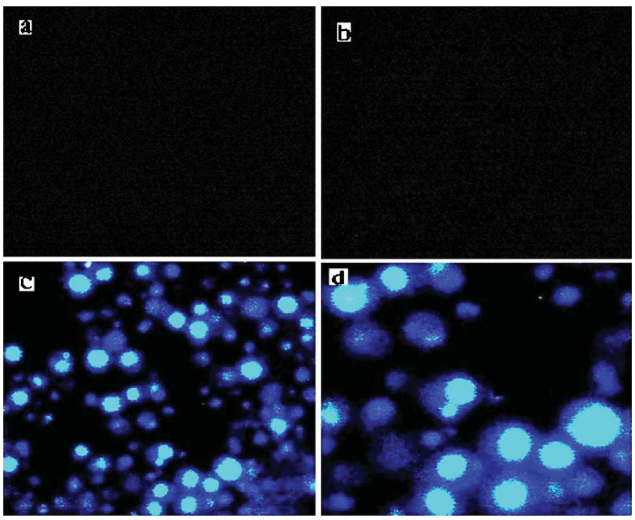

Fig. 11 Fluorescence microscopy images of *Candida albicans* cells (IMTECH No. 3018): image of *Candida albicans* without **L** (a), cells loaded with probe **L** (10 μM) for 30 min under 100× objective lens (b), fluorescence image of **L**-stained *Candida albicans* cells pre-exposed to 10 μM Al^{3+} for 30 min under 100× objective lens (c), magnified view of c (d). Incubation was performed at 37 °C.

From Fig. 11, we could conclude that (i) only Al^{3+} pre-treated cells had been stained by **L**, (ii) **L** was easily permeable through the cell membrane without causing any harm as the cells remained alive even after 30 min of exposure to **L** at 10 μM. Thus, **L** could detect intracellular Al^{3+} in living cells very efficiently.

Experimental section

Materials and methods

High-purity HEPES, 2-hydroxy naphthaldehyde and diethylenetriamine were purchased from Sigma Aldrich (India). $Al(NO_3)_3{\cdot}9H_2O$ was purchased from Merck (India). Solvents used were of spectroscopic grade. Other chemicals were of analytical reagent grade and had been used without further purification except when specified. Mili-Q Milipore® 18.2 MΩ cm^{-1} water was used throughout all the experiments. A JASCO (model V-570) UV-Vis spectrophotometer was used for recording UV-Vis spectra. FTIR spectra were recorded on a JASCO FTIR spectrophotometer (model: FTIR-H20). Mass spectra were performed on a QTOF Micro YA 263 mass spectrometer in ES positive mode. Thermo gravimetric analyses were performed on a Perkin Elmer TG/DTA lab system 1 (Technology by SII). ^1H NMR spectra were recorded using a Bruker Avance 600 (600 MHz) in DMSO-d_6. Elemental analysis was performed using a Perkin Elmer CHN-Analyzer with a first 2000-Analysis kit. The steady-state fluorescence emission and excitation spectra were recorded with a Hitachi F-4500 spectrofluorimeter. All pH measurements were performed with a Systronics digital pH meter (model 335). All spectra were recorded at room temperature except for fluorescence microscopy images.

Imaging system

The imaging system comprised of an inverted fluorescence microscope (Leica DM 1000 LED), digital compact camera (Leica DFC 420C), and an image processor (Leica Application Suite v3.3.0). The microscope was equipped with a mercury 50 W lamp.

Synthesis of *N*-(2-hydroxy-1-naphthalene)-*N*′-(2-(2-hydroxy-1-naphthalene)amino-ethyl)-ethane-1,2-diamine (L)

An ethanol solution of 2-hydroxy naphthaldehyde (1 g, 5.81 mmol) was added dropwise to a solution (30 mL) of diethylenetriamine (0.314 mL, 2.905 mmol) in ethanol under stirring condition at room temperature (Scheme 1). Stirring was continued for a further 30 min followed by reflux for 8 h. Upon removal of the solvent, a yellow colored residue was obtained. The residue was recrystallized from ethanol. Yield 82%; mp: 145 °C (± 4 °C); ^1H NMR (600 MHz, DMSO-d_6) (Fig. S1, ESI†): 2.9 (4H, t, J = 6.0 Hz); 3.7 (4H, q, J = 5.4 Hz); 6.7 (2H, d, J = 9.6 Hz); 7.15 (2H, t, J = 7.2 Hz); 7.4 (2H, m, J = 7.2 Hz); 7.6 (2H, d, J = 9 Hz); 7.7 (2H, d, J = 9 Hz); 8.0 (2H, d, J = 8.4 Hz); 9.1 (2H, d, J = 10.2 Hz); 13.9 (2H, s); QTOF-MS ES^+ (Fig. S2, ESI†): $[M+Na]^+$ = 434.21; elemental analysis data as calculated for $C_{26}H_{25}N_3O_2$(%): C, 75.89; H, 6.12; N, 10.21. Found (%): C, 75.72; H, 6.03; N, 10.15. FTIR (cm^{-1}) (Fig. S4, ESI†): ν(NH) 3448.07, ν(OH) 3301.3, ν(C═N) 1629.7.

Synthesis of [Al(L)(NO_3)]

A 10 mL methanol solution of $Al(NO_3)_3{\cdot}9H_2O$ (0.182 g, 0.486 mmol) was added slowly to a magnetically stirred solution (10 mL) of the ligand (**L**) (0.2 g, 0.4866 mmol) in methanol. Stirring was continued for 6 h. On slow evaporation of the solvent, an off-white colored compound was obtained. The compound was collected from methanol. QTOF-MS ES^+ (Fig. S3, ESI†): $[M+Na]^+$ = 523.19. FTIR (cm^{-1}) (Fig. S9, ESI†): ν(NH) 3449.17, ν(OH), 3449.17; ν(C═N), 1619.22; ν(-NO_3^-), 1385.15. ^1H NMR (600 MHz, DMSO-d_6) (Fig. S10, ESI†).

Preparation and imaging of cells

Candida albicans cells (IMTECH No. 3018) from an exponentially growing culture in yeast extract glucose broth medium (pH 6.0, incubation temperature, 37 °C) were centrifuged at 3000 rpm for 10 min, washed twice with 0.1 M HEPES buffer (pH 7.4). Then cells were treated with different concentrations of Al^{3+} (from 5 μM to 10 μM) for 30 min in 0.1 M HEPES buffer (pH 7.4) containing 0.01% Triton X100 as permeability enhancing agent. After incubation, the cells were washed with HEPES buffer and incubated with **L** (10 μM) for 15 min. Cells obtained were mounted on grease-free glass slides and observed under the fluorescence microscope equipped with a UV filter. Cells incubated with **L** but without Al^{3+} were used as control.

Both Al^{3+} treated and untreated cells were stained with **L** and observed under the fluorescence microscope.

Conclusion

A facile one-step synthesis of a naphthalene-based Al^{3+} chemosensor (**L**) was described. **L** could detect Al^{3+} in ethanol as well as in HEPES buffer. Detection of Al^{3+} by **L** was not limited to abiotic systems but also extended to living cells at physiological pH. Fluorescence enhancement of **L** after addition of Al^{3+} was attributed to the absence of ICT, restricted rotation and increasing

CHEF effect. Plausible accompanying cations did not interfere in the detection of Al^{3+}. This new Al^{3+} selective fluorescent probe may find potential bio-medical applications.

Acknowledgements

We are grateful to the West Bengal Council of Science and Technolgy (DST, Govt. of West Bengal) for funding. A. Sahana, S. Lohar and D. Karak are thankful to CSIR and UGC, New Delhi for providing fellowship. The authors thank the Indian Institute of Chemical Biology (IICB), Kolkata for extending NMR and mass spectrometer facilities. We also thank the University Science Instrumentation Center (USIC), Burdwan University for providing the fluorescence microscope facility. The authors thank the learned referees.

Notes and references

1 J. R. J. Sorenson, I. R. Campbell, L. B. Tepper and R. D. Lingg, *Environ. Health Perspect.*, 1974, **8**, 3.
2 V. K. Gupta, A. K. Jain and G. Maheshwari, *Talanta*, 2007, **72**, 1469; T. P. Flaten, *Brain Res. Bull.*, 2001, **55**, 187.
3 E. Delhaize and P. R. Ryan, *Plant Physiol.*, 1995, **107**, 315; D. L. Godbold, E. Fritz and A. Huttermann, *Proc. Natl. Acad. Sci. USA*, 1988, **85**, 3888.
4 J. Barcelo and C. Poschenrieder, *Environ. Exp. Bot.*, 2002, **48**, 75; B. Valeur and I. Leray, *Coord. Chem. Rev.*, 2000, **205**, 3; Z. Krejpcio and R. W. P. J. Wojciak, *Environ. Studies*, 2002, **11**, 251.
5 M. B. Saleh, S. S. M. Hassan, A. A. A. Gaber and N. A. A. Kream, *Anal. Chim. Acta*, 2001, **434**, 247; S. Zareba and J. Melke, *Pharm. Acta Helv.*, 2000, **74**, 361; A. J. Downard, B. O'Sullivan and K. J. Powell, *Polyhedron*, 1996, **15**, 3469; H. Lian, Y. Kang, S. Bi, Y. Arkin, D. Shao, D. Li, Y. Chen, L. Dai, N. Gan and L. Tian, *Talanta*, 2004, **62**, 43.
6 L. Wang, W. Qin, X. Tang, W. Dou, W. Liu, Q. Teng and X. Yao, *Org. Biomol. Chem.*, 2010, **8**, 3751; K. K. Upadhyay and A. Kumar, *Org. Biomol. Chem.*, 2010, **8**, 4892; D. Maity and T. Govindaraju, *Chem. Commun.*, 2010, **46**, 4499; M. Arduini, F. Felluga, F. Mancin, P. Rossi, P. Tecilla, U. Tonellato and N. Valentinuzzi, *Chem. Commun.*, 2003, 1606; D. Maity and T. Govindaraju, *Inorg. Chem.*, 2010, **49**, 7229; Y. W. Wang, M. X. Yu, Y. H. Yu, Z. P. Bai, Z. Shen, F. Y. Li and X. Z. You, *Tetrahedron Lett.*, 2009, **50**, 6169.
7 K. Soroka, R. S. Vithanage, D. A. Phillips, B. Walker and P. K. Dasgupta, *Anal. Chem.*, 1987, **59**, 629.
8 J. M. Cano-pavón, M. L. Trujillo and A. García De Torres, *Anal. Chim. Acta*, 1980, **117**, 319; M. P. Mánuel-Vez and M. García-Vargas, *Talanta*, 1994, **41**, 1553; F. dePablos, J. L. G. Ariza and F. Pino, *Analyst*, 1986, **111**, 1159; C. Jiang, B. Tang, R. Wang and J. Yen, *Talanta*, 1997, **44**, 197.
9 J.-Q. Wang, L. Huang, L. Gao, J. H. Zhu, Y. Wang, X. Fan and Z. Zou, *Inorg. Chem. Commun.*, 2008, **11**, 203; M. S. J. Briggs, J. S. Fossey, C. J. Richards, B. Scotta and John Whateleya, *Tetrahedron Lett.*, 2002, **43**, 5169; S. D. Kim, D. H. Lee and J. S. Kim, *Bull. Korean Chem. Soc.*, 2008, **29**, 245.
10 Y. O. Lee, Y. H. Choi and J. S. Kim, *Bull. Korean Chem. Soc.*, 2007, **28**, 151; A. B. Othman, J. W. Lee, Y.-D. Huh, R. Abidi, J. S. Kimd and J. Vicens, *Tetrahedron*, 2007, **63**, 10793.
11 R. S. Sathish, A. G. Raju, G. N. Rao and C. Janardhana, *Spectrochim. Acta, Part A*, 2008, **69**, 282; S. Sathish, G. Narayan, N. Rao and C. Janardhana, *J. Fluoresc.*, 2006, **17**, 1.
12 Y. Zhao, Z. Lin, H. Liao, C. Duan and Q. Meng, *Inorg. Chem. Commun.*, 2006, **9**, 966.
13 A. Jeanson and V. Be'reau, *Inorg. Chem. Commun.*, 2006, **9**, 13.
14 S. M. Z. Al-Kindy, F. E. O. Suliman and A. E. Pillay, *Instrum. Sci. Technol.*, 2006, **34**, 619; J. L. Ren, J. Zhang, J. Qing Luo, X. K. Pei and Z. Xi Jiang, *Analyst*, 2001, **126**, 698; S. M. Ng and R. Narayanaswamy, *Anal. Bioanal. Chem.*, 2006, **386**, 1235.
15 N. Chattopadhyay, A. Mallick and S. Sengupta, *J. Photochem. Photobiol., A*, 2006, **177**, 55; Y. G. Zhao, Z. H. Lin, H. P. Liao, C. Y. Duan and Q. J. Meng, *Inorg. Chem. Commun.*, 2006, **9**, 966.
16 L. Salmon, P. Thury, E. Rivi'ere and M. Ephritikhine, *Inorg. Chem.*, 2006, **45**, 83; D. M. Epstein, S. Choudhary, M. R. Churchill, K. M. Keil, A. V. Eliseev and J. R. Morrow, *Inorg. Chem.*, 2001, **40**, 1591.
17 V. C. Da Silveira, J. S. Luz, C. C. Oliveira, I. Graziani, M. R. Ciriolo and A. M. Ferreira, *J. Inorg. Biochem.*, 2008, **102**, 1090.
18 S. Padhye and G. B. Kauffman, *Coord. Chem. Rev.*, 1985, **63**, 127; Y. Li and Z. Y. Yang, *Inorg. Chim. Acta*, 2009, **362**, 4823.
19 S. Kasselouri, A. Garoufis, A. Katehanakis, G. Kalkanis, S. P. Perlepes and N. Hadjiliadis, *Inorg. Chim. Acta*, 1993, **207**, 255.
20 D. P. Roek, J. E. Chateauneuf and J. F. Brennecke, *Ind. Eng. Chem. Res.*, 2000, **39**, 3090.
21 P. Frederick and S. P. Schwarz Wasik, *Anal. Chem.*, 1976, **48**, 524.
22 M. Ali, M. Jha, S. K. Das and S. K. Saha, *J. Phys. Chem. B*, 2009, **113**, 15563.
23 (*a*) M. Shortreed, R. Kopelman, M. Kuhn and B. Hoyland, *Anal. Chem.*, 1996, **68**, 1414; (*b*) A. Caballero, R. Martinez, V. Lloveras, I. Ratera, J. Vidal-Gancedo, K. Wurst, A. Tárraga, P. Molina and J. Veciana, *J. Am. Chem. Soc.*, 2005, **127**, 15666.
24 M. Cametti, A. Dalla Cort, M. Colapietro, G. Portalone, L. Russo and K. Rissanen, *Inorg. Chem.*, 2007, **46**, 9057; A. Ben Othman, J. W. Lee, Y. D. Huh, R. Abidi, J. S. Kim and J. Vicens, *Tetrahedron*, 2007, **63**, 10793.